PCCP

PAPER

View Article Online
View Journal | View Issue

Cite this: *Phys. Chem. Chem. Phys.*, 2016, **18**, 25569

Proton transfer in acetaldehyde–water clusters mediated by a single water molecule†

Oleg Kostko,* Tyler P. Troy, Biswajit Bandyopadhyay and Musahid Ahmed

Received 15th July 2016,
Accepted 26th August 2016

DOI: 10.1039/c6cp04916h

www.rsc.org/pccp

Proton transfer in aqueous media is a ubiquitous process, occurring in acid–base chemistry, biology, and in atmospheric photochemistry. Photoionization mass spectrometry coupled with theoretical calculations demonstrate that a relay-type proton transfer mechanism is operational for single-water-molecule-assisted proton transfer between two acetaldehyde molecules in the gas phase. Threshold photoionization of acetaldehyde–water clusters leads to proton transfer between the formyl groups (–CH═O) of one acetaldehyde molecule to another, and the subsequent formation of cationic moieties. Density functional theory computations reveal several plausible pathways of proton transfer in mixed cluster cations. Among these pathways, water-mediated proton transfer is energetically favored. Mass spectra and photoionization efficiency curves confirm these theoretical findings and also demonstrate the increased stability of cluster cations where acetaldehyde molecules are symmetrically bonded to the hydronium ion.

Introduction

Water is ubiquitous on Earth driving numerous important chemical reactions, on both macro and molecular scales. Proton transfer (PT) in aqueous media is one such process and is a fundamental reaction in biological systems,[1] electrochemistry,[2–4] and atmospheric photochemistry.[5–7] A detailed understanding of PT is crucial for the design of proton-exchange membranes used in the construction of efficient fuel cells.[3,4] Inside biological systems, water is confined within nano-channels and may act as water wires. For instance, a proton is transferred to the protein interior through a chain of water molecules inside of Rhodobacter sphaeroides.[1] Lengthy H-bonded networks between amino acids and water molecules were found in the extracellular region of bacteriorhodopsin.[1] Single-molecule-mediated PT is not only found in biology. A single OH-terminated atomic defect of graphene has been observed to transfer water's proton through a single graphene layer.[8] A single water molecule has also been demonstrated to mediate PT accepting a proton from one molecule and donating it to another.[9]

Acetaldehyde plays a significant role in tropospheric chemistry[10] and is a carcinogenic air pollutant.[11] Acetaldehyde can exist in two isomeric forms: keto and enol in the gas phase, which has been investigated both *via* experiment and theory.[12–14] For the neutral acetaldehyde molecule, keto–enol isomerization is endothermic by 9.9 kcal mol^{-1}. In contrast, the process in the ionized system is exothermic by about 17.1 kcal mol^{-1}.[12] Investigations of ionized acetaldehyde have shown that the assistance of one or more solvent molecules enables proton transfer from a methyl group to oxygen and thus significantly decreases the energy barrier to isomerization.[12,13] It was also shown that methanol is a better catalyst than water for proton transfer.[12] In the case of the reaction of the acetaldehyde cation with methanol, the isomerization to a vinyl alcohol is shown to be a barrierless process.[12] A water molecule can catalyze the oxidation reaction of acetaldehyde by a hydroxyl radical,[15] though this result has been recently contradicted.[16] Di Palma and Bende used tunable radiation to probe tautomerism in acetaldehyde–water clusters, however interpretation did not extend to probing the PT dynamics in this particular system.[17] Here, we present tunable vacuum ultraviolet (VUV) photoionization mass spectrometry coupled with density functional theory (DFT) to reveal single-water-molecule-mediated PT in mixed acetaldehyde–water clusters.

Experimental and computational methods

The experiment was performed on a molecular beam apparatus coupled to a 3m monochromator at the Chemical Dynamics beamline (9.0.2) at the Advanced Light Source, Lawrence Berkeley National Laboratory.[18,19] Acetaldehyde and acetaldehyde–water clusters were generated *via* expansion of 300 Torr of 2% acetaldehyde in helium and water–argon mixtures through a 100 μm orifice. Neutral species were skimmed before ionization by

Chemical Sciences Division, Lawrence Berkeley National Laboratory, Berkeley, CA 94720, USA. E-mail: okostko@lbl.gov

† Electronic supplementary information (ESI) available: Geometries and energetics of all considered in the paper clusters; optimized Cartesian coordinates of the clusters. See DOI: 10.1039/c6cp04916h

tunable synchrotron VUV radiation in the interaction region of a reflectron time-of-flight (TOF) mass spectrometer. TOF mass spectra were measured for photon energies in the range 8.0 to 11.3 eV at 0.05 eV increments. The PIE curves were obtained by integrating over the mass peaks at each photon energy and normalizing with respect to photon flux measured by a silicon photodiode.

Calculations were performed using the Gaussian 09 package.[20] Neutral structures were optimized at the B3LYP/6-31g(d) level and final geometry optimizations and frequency calculations were performed using the long-range and dispersion-corrected ωB97X-D functional with a 6-311+G(d,p) basis set. Frequency calculations allowed identification of stationary points. Adiabatic ionization energies (aIEs) were obtained from the differences in the zero-point corrected electronic energies for each neutral cluster and its corresponding cation. Vertical ionization energies (vIEs) were computed by single-point energy calculations of the cations at the respective neutral ground-state geometries. This method has demonstrated in thermochemical computations accuracies within 3.37 kcal mol^{-1}.[21,22]

Results and discussions

The photoionization mass spectrum of gas-phase acetaldehyde–water mixture, generated *via* a supersonic molecular beam expansion, shows a strong monomer cation peak followed by two series of peaks: protonated acetaldehyde cluster cations ($A_n{\cdot}H^+$) and protonated acetaldehyde–water ($A_nH{\cdot}H_2O^+$) complexes. The mass spectrum obtained at 10.5 eV photon energy, which is above the ionization energy of acetaldehyde monomer (10.23 eV),[23] is shown in Fig. 1. Protonated acetaldehyde–water cluster cations are less abundant than the protonated acetaldehyde species since the water content of the molecular beam is small.

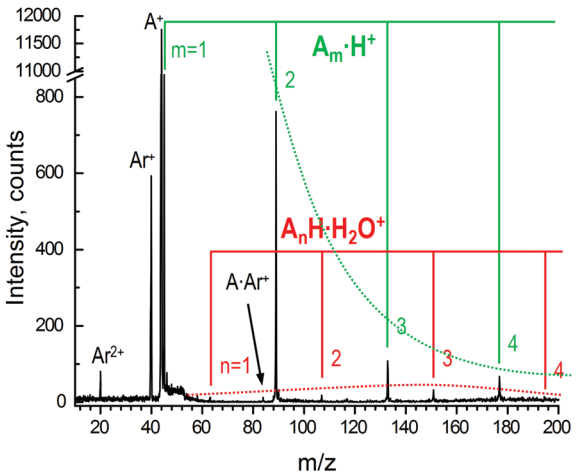

Fig. 1 Photoionization time-of-flight mass spectrum of acetaldehyde–water complexes (A_mH^+ and $A_nH{\cdot}H_2O^+$), measured at 10.5 eV photon energy. Two series of peaks detected in the experiments are color coded: green corresponds to protonated bare acetaldehyde clusters (A_mH^+), red peaks represent protonated acetaldehyde–water ($A_nH{\cdot}H_2O^+$) complexes. Dashed lines demonstrate intensity trends for A_mH^+ and $A_nH{\cdot}H_2O^+$ species. Ar^+ and Ar_2^+ peaks appear due to high harmonic ionization of argon which is used as carrier gas. The small peak at m/z = 84 corresponds to the acetaldehyde–argon ion complex.

As a general case, the ionization of hydrogen-bonded clusters leads to the formation of cluster cations (acetaldehyde, A_n^+) or protonated cations ($A_n{\cdot}H^+$) according to the following reactions:

$$A_n + h\nu \rightarrow A_n^+ + e^- \quad (1)$$

$$A_n + h\nu \rightarrow A_n^{+*} + e^- \rightarrow A_{n-1}^+ + A + e^- \quad (2)$$

$$A_n + h\nu \rightarrow A_n^{+*} + e^- \rightarrow A_{n-1}{\cdot}H^+ + (A\text{–}H)^\bullet + e^- \quad (3)$$

In reactions (2) and (3) Franck–Condon ionization leads to excited state(s) of cation (A^{+*}), which dissociates into smaller species. The mass spectrum in Fig. 1 suggests that reactions (1) and (2) do not occur efficiently since larger non-protonated ionic species are not detected apart from the monomer and small traces of the dimer. Therefore, only reaction (3) produces the observed protonated acetaldehyde cations. Likewise, protonated acetaldehyde–water complexes are formed by the following reactions:

$$A_n{\cdot}H_2O + h\nu \rightarrow A_n{\cdot}H_2O^{+*} + e^- \rightarrow A_{n-1}H{\cdot}H_2O^+ + (A\text{–}H)^\bullet + e^- \quad (4)$$

Previously, it was observed that fragmentation of hydrogen-bonded clusters by evaporation of more than one monomer is insignificant.[24]

Comparison of the peak intensity distributions for ($A_n{\cdot}H^+$) and ($A_nH{\cdot}H_2O^+$) species (Fig. 1) shows that protonated acetaldehyde cluster intensity (green dashed line) exponentially decreases with increasing n. This distribution agrees with a model describing cluster growth in supersonic expansions whereby the collisions between gas molecules lead to the formation of dimers and to the sequential growth of larger clusters *via* collisions with surrounding molecules.[25] A drop in gas density after the supersonic expansion leads to the prevalence of smaller species and an exponentially decreasing population of larger clusters. In contrast, the distribution of protonated acetaldehyde–water cluster cations is different; where rather the protonated trimer-water ($A_3H{\cdot}H_2O^+$) shows the maximum intensity. This behavior cannot be simply explained by a growth mechanism of the clusters, as in the case of $A_n{\cdot}H^+$ species.

In an attempt to explain the intensity distribution and to understand the cluster formation mechanisms, theoretical calculations were performed for the acetaldehyde–water complexes. To decipher the formation of $AH{\cdot}H_2O^+$ species using DFT calculations, a number of initial neutral acetaldehyde dimer–water structures are considered (see ESI† for details). Here we discuss in detail those three representative photoionization processes depicted in Fig. 2.

Three general structural trends are observed in neutral species. In one case a water molecule bonds to two acetaldehyde moieties, as shown in Fig. 2(IIIa). Though the $A_2{\cdot}H_2O$ clusters shown in Fig. 2(Ia) and (IIa) look quite similar, the difference becomes apparent after an analysis of intermolecular distances. In both cases, one acetaldehyde is more strongly bound to water than another (the bond length between the stronger bound

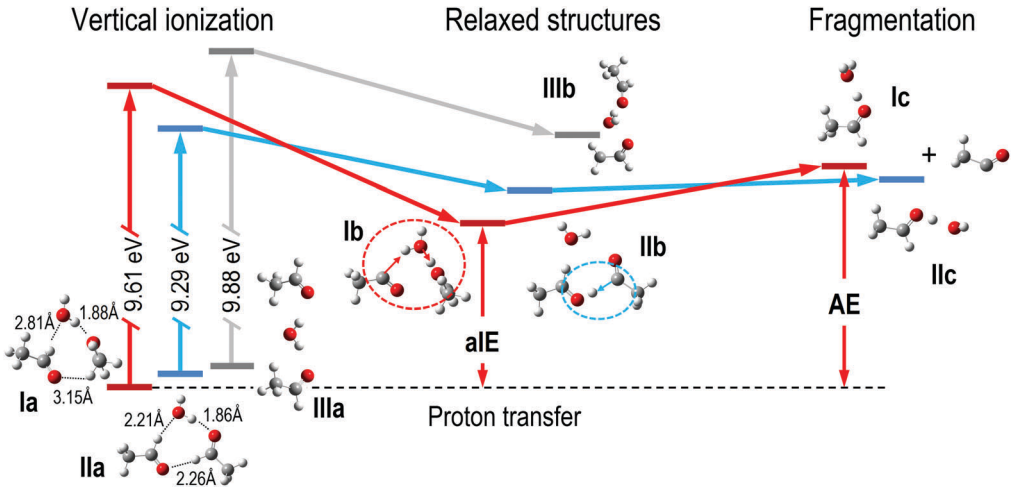

Fig. 2 Schematic energy diagram for the ionization and fragmentation of three different isomers of acetaldehyde dimer–water complexes. The adiabatic ionization energy (aIE) and appearance energy (AE) is shown only for structure I.

acetaldehyde and water is about 1.87 Å). The weaker bound acetaldehyde is further from acetaldehyde–water pair in case (Ia), being substantially closer to water than to another acetaldehyde moiety (see intermolecular distances in Fig. 2Ia). For structure (IIa), the weaker bound acetaldehyde is almost equidistant to both water and another acetaldehyde. The neutral structure (Ia) is the energetically most favorable structure, lying 39 meV below structure (IIa). Structure (IIIa) is the least favorable, lying 75 meV above the isomer (Ia). Strong adiabatic cooling in a supersonic expansion of a molecular beam leads to preferential population of the most stable isomer, (Ia) in this case.

Vertical ionization of neutral $A_2{\cdot}H_2O$ clusters leads to excess internal energy in the system and subsequent geometry relaxation. Examination of the cations (Fig. 2) leads to an understanding of the different dynamics at play for the three above-mentioned cases. Case (IIIb) does not occur, since the intact $A_2{\cdot}H_2O^+$ cation is not detected in the mass spectrum. In case (IIb), the proton transfers from a formyl group of one acetaldehyde to another (the direction of proton movement is indicated with a blue arrow in Fig. 2IIb), similar to the case of pure acetaldehyde clusters.[17] Case (Ib) is the most interesting under which a water molecule participates in PT from one acetaldehyde to another. Here, water forms a "relay-type" transport of protons, resembling the Grotthuss mechanism,[26] where rapid exchange between a covalent and hydrogen bond takes place between two adjacent acetaldehydes (see red arrows depicting the proton movement direction in Fig. 2Ib).

Absorption of a VUV photon by neutral $A_2{\cdot}H_2O$ structures (I) and (II) induces vertical ionization to the cationic state. Charge redistributions in the structures lead to barrierless PT, followed by spontaneous fragmentation (see Fig. 2Ic and IIc), since the excess energy gained during vertical ionization is sufficient to overcome the small dissociation barrier and to form the experimentally detected $AH{\cdot}H_2O^+$ cations.

Photoionization efficiency (PIE) curves (providing information on ionization and/or fragmentation energetics) were measured to quantify which neutral structures populate the molecular beam. A PIE curve for the protonated acetaldehyde–water monomer is shown in Fig. 3(a) together with the PIE curve for $AH{\cdot}D_2O^+$ distinguished by a dotted line. An experiment with deuterated water (D_2O) was conducted to test where the proton in $A_nH{\cdot}H_2O^+$ cations is sourced – from acetaldehyde or from another water molecule. In that experiment, the peaks observed in the mass spectrum corresponding to protonated acetaldehyde–water complexes, are shifted by 2 amu, in accordance to formula $A_nH{\cdot}D_2O^+$. The appearance energy (AE, mass signal onset) for m/z = 63 ($AH{\cdot}H_2O^+$) may be determined from the PIE curve to be 9.78 ± 0.10 eV. The PIE curve for the deuterated experiment, m/z = 65 ($AH{\cdot}D_2O^+$) demonstrates an excellent correlation with that of m/z = 63, confirming that the proton is coming from another acetaldehyde moiety and therefore that the energetics in both cases are similar.

The computed vIEs for all examined cluster isomers are shown in Fig. 3(a) for both cases: water mediated PT (case I above) and direct PT between acetaldehydes (conventional PT, case II). A good correlation of the experimental onset with the computed vertical ionization energy suggests that the Franck–Condon factors are unfavorable for an adiabatic transition, which is about 1 eV lower than the vertical ionization energy (see Table 1 and Table S1 in the ESI†) and therefore only a vertical transition is observed experimentally. The PIE curve onset (9.78 ± 0.10 eV) and the theoretical vIE value, corresponding to the water-mediated case of 9.61 eV (9.62 eV for $A_2{\cdot}D_2O^+$ species) are in excellent agreement. The agreement of the theoretical vIE with the experimental AE, coupled with the fact that the neutral structure (I) is the most energetically favorable, confirms that the water molecule mediates PT under these experimental conditions.

The experimental value of the appearance energy for the $A_2H{\cdot}H_2O^+$ cation, determined from the PIE curve shown in Fig. 3(b) is 9.45 ± 0.10 eV. The DFT calculations for $A_3{\cdot}H_2O$, similar to the case of $A_2{\cdot}H_2O$ ionization, reveal three different scenarios for what could occur upon ionization: (a) $A_3{\cdot}H_2O$ ionizes intact, (b) proton

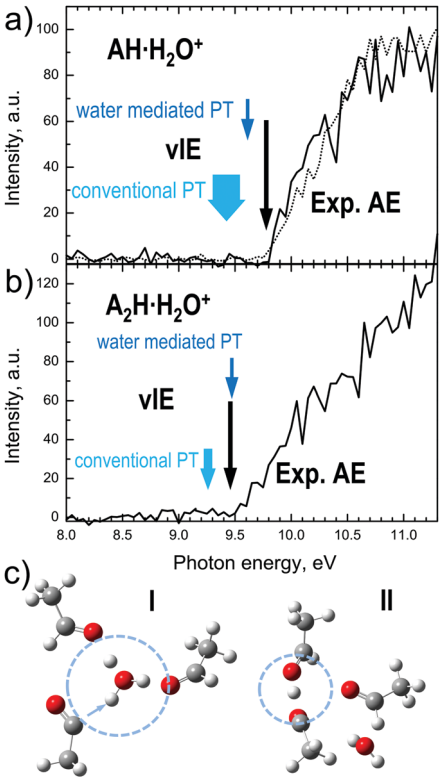

Fig. 3 (a) Photoionization efficiency (PIE) curve for $AH{\cdot}H_2O^+$ (m/z = 63). The dotted line in the panel corresponds to PIE signal from m/z = 65 ($AH{\cdot}D_2O^+$). (b) The PIE curve for $A_2H{\cdot}H_2O^+$ (m/z = 107). The black arrows in panels (a) and (b) denote the experimental PIE onsets. Blue arrows denote theoretical energy ranges obtained for vertical ionization energies, corresponding to different PT processes in $A_n{\cdot}H_2O$ clusters. (c) Two examples of proton-transferred acetaldehyde trimer–water complexes.

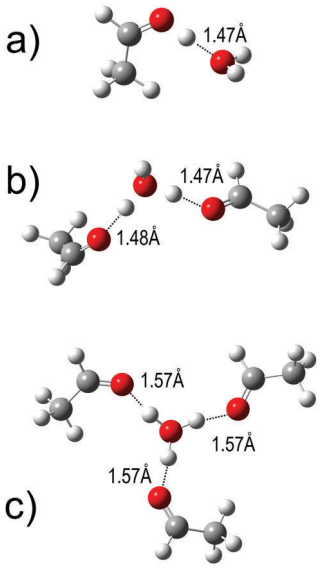

Fig. 4 DFT computed structures for (a) $AH{\cdot}H_2O^+$, (b) $A_2{\cdot}H_3O^+$, and (c) $A_3{\cdot}H_3O^+$ structures, for which water-mediated proton transfer is observed.

transfers from one acetaldehyde to another followed by fragmentation and (c) proton transfer is mediated by water. Two examples of cases (b) and (c) are shown in Fig. 3(c). The acetaldehyde–water complex, shown in Fig. 3(c, I), corresponds to case (c) where water is mediating PT from one acetaldehyde to another. Again, as in the case of $AH{\cdot}H_2O^+$ formation, the neutral parent $A_3{\cdot}H_2O$ molecule, corresponding to the case (c) is the lowest in energy, being 12–55 meV below the examined proton-transferred cases (b) and 55–57 meV below the ionized intact complexes (see Table S1 in ESI†). This suggests that under molecular beam conditions, the most stable structure, shown in Fig. 3(c, I) is dominant. An excellent agreement of the calculated vIE for case (c) with the observed experimental onset (9.47 and 9.45 ± 0.10 eV, respectively) further bolsters the case that for the acetaldehyde trimer–water cluster, water mediated PT again dominates upon cluster ionization.

The structures of protonated cations of the most stable acetaldehyde–water complexes where PT is mediated by water are shown in Fig. 4. In two of the three presented cases, the acetaldehyde molecules are bound to a hydronium ion (H_3O^+), creating structures with the formulas $A_2{\cdot}H_3O^+$, and $A_3{\cdot}H_3O^+$. While in the case of $AH{\cdot}H_2O^+$ the proton is closer to acetaldehyde's oxygen, for $A_3{\cdot}H_3O^+$, the hydronium ion and all three surrounding acetaldehydes are equidistant (see Fig. 4c, the bond lengths between the acetaldehydes and hydronium are 1.57 Å). The high symmetricity of the $A_3{\cdot}H_3O^+$, whereby the acetaldehyde fills up the solvation shell, makes the cation the most stable and the most abundant in the mass spectrum (Fig. 1). Appearance of such structure-driven magic numbers has been previously observed *e.g.* for alcohol–water clusters.[27] In the latter case, the energetically stable clusters prefer to maximize the number of hydrogen bonds and minimize the distance between the alcohol molecules and the ion core.

Table 1 Adiabatic and vertical ionization energies (aIEs, vIEs), and appearance energies (AE) for DFT computed structures compared with experimental AEs. Three different ionization processes are presented: direct ionization (DI), conventional PT (cPT), and water mediated PT (WmPT)

Parent	Type of ionization	aIE, eV	vIE, eV	AE, eV	Detection channel	m/z	Exp. AE, eV
$A_2{\cdot}H_2O$	cPT	8.43–8.44	9.29–9.56	8.65–9.21	$AH{\cdot}H_2O^+$	63	9.78 ± 0.10
	WmPT	8.21	9.61	8.74			
	DI	8.96–9.00	9.78–9.88	—	$A_2{\cdot}H_2O^+$	106	—
$A_2{\cdot}D_2O$	cPT	8.43–8.44	9.29–9.57	8.65–9.18	$AH{\cdot}D_2O^+$	65	9.75 ± 0.10
	WmPT	8.21	9.62	8.74			
$A_3{\cdot}H_2O$	cPT	7.72–8.20	9.22–9.29	8.04–8.33	$A_2H{\cdot}H_2O^+$	107	9.45 ± 0.10
	WmPT	8.51	9.47	8.90			
	DI	8.53	9.38–9.39	—	$A_3{\cdot}H_2O^+$	150	—
$A_4{\cdot}H_2O$	WmPT	8.32	9.16	8.52	$A_3H{\cdot}H_2O^+$	151	9.40 ± 0.20

Conclusions

We carried out experimental and theoretical investigations of mixed acetaldehyde–water clusters and found an increased stability of the protonated acetaldehyde trimer–water cluster. This work provides new insight into proton transfer mechanisms whereby a single water molecule can lead to the formation of more stable acetaldehyde–water clusters, which upon ionization, transfer a proton from one acetaldehyde to another with the assistance of water.

Acknowledgements

This work and the Advanced Light Source are supported by the Director, Office of Science, Office of Basic Energy Sciences, of the U.S. Department of Energy under Contract No. DE-AC02-05CH11231, through the Chemical Sciences Division.

References

1 S. Cukierman, *Biochim. Biophys. Acta, Bioenerg.*, 2006, **1757**, 876–885.
2 K.-D. Kreuer, S. J. Paddison, E. Spohr and M. Schuster, *Chem. Rev.*, 2004, **104**, 4637–4678.
3 K. Schmidt-Rohr and Q. Chen, *Nat. Mater.*, 2008, **7**, 75–83.
4 R. Devanathan, *Energy Environ. Sci.*, 2008, **1**, 101–119.
5 S. Aloisio and J. S. Francisco, *Acc. Chem. Res.*, 2000, **33**, 825–830.
6 R. B. Gerber, M. E. Varner, A. D. Hammerich, S. Riikonen, G. Murdachaew, D. Shemesh and B. J. Finlayson-Pitts, *Acc. Chem. Res.*, 2015, **48**, 399–406.
7 V. Vaida, *J. Chem. Phys.*, 2011, **135**, 20901.
8 J. L. Achtyl, R. R. Unocic, L. Xu, Y. Cai, M. Raju, W. Zhang, R. L. Sacci, I. V. Vlassiouk, P. F. Fulvio, P. Ganesh, D. J. Wesolowski, S. Dai, A. C. T. van Duin, M. Neurock and F. M. Geiger, *Nat. Commun.*, 2015, **6**, 6539.
9 T. Loerting and K. R. Liedl, *J. Phys. Chem. A*, 2001, **105**, 5137–5145.
10 B. J. Finlayson-Pitts and J. N. Pitts Jr., *Chemistry of the Upper and Lower Atmosphere*, Academic Press, San Diego, 2000, pp. 547–656.
11 Y. Zhou, C. Li, M. A. J. Huijbregts and M. M. Mumtaz, *PLoS One*, 2015, **10**, e0140013.
12 L. Rodríguez-Santiago, O. Vendrell, I. Tejero, M. Sodupe and J. Bertran, *Chem. Phys. Lett.*, 2001, **334**, 112–118.
13 G. van der Rest, H. Nedev, J. Chamot-Rooke, P. Mourgues, T. B. McMahon and H. E. Audier, *Int. J. Mass Spectrom.*, 2000, **202**, 161–174.
14 X. Wang, W. Sun and J. L. Holmes, *J. Phys. Chem. A*, 2006, **110**, 8409–8417.
15 E. Vöhringer-Martinez, B. Hansmann, H. Hernandez, J. S. Francisco, J. Troe and B. Abel, *Science*, 2007, **315**, 497–501.
16 C. Iuga, J. R. Alvarez-Idaboy, L. Reyes and A. Vivier-Bunge, *J. Phys. Chem. Lett.*, 2010, **1**, 3112–3115.
17 T. M. Di Palma and A. Bende, *J. Mass Spectrom.*, 2014, **49**, 700–708.
18 A. Golan, K. B. Bravaya, R. Kudirka, O. Kostko, S. R. Leone, A. I. Krylov and M. Ahmed, *Nat. Chem.*, 2012, **4**, 323–329.
19 F. Bell, Q. N. Ruan, A. Golan, P. R. Horn, M. Ahmed, S. R. Leone and M. Head-Gordon, *J. Am. Chem. Soc.*, 2013, **135**, 14229–14239.
20 M. J. Frisch, G. W. Trucks, H. B. Schlegel, G. E. Scuseria, M. A. Robb, J. R. Cheeseman, G. Scalmani, V. Barone, B. Mennucci, G. A. Petersson, H. Nakatsuji, M. Caricato, X. Li, H. P. Hratchian, A. F. Izmaylov, J. Bloino, G. Zheng, J. L. Sonnenberg, M. Hada, M. Ehara, K. Toyota, R. Fukuda, J. Hasegawa, M. Ishida, T. Nakajima, Y. Honda, O. Kitao, H. Nakai, T. Vreven, J. A. Montgomery Jr., J. E. Peralta, F. Ogliaro, M. J. Bearpark, J. Heyd, E. N. Brothers, K. N. Kudin, V. N. Staroverov, R. Kobayashi, J. Normand, K. Raghavachari, A. P. Rendell, J. C. Burant, S. S. Iyengar, J. Tomasi, M. Cossi, N. Rega, N. J. Millam, M. Klene, J. E. Knox, J. B. Cross, V. Bakken, C. Adamo, J. Jaramillo, R. Gomperts, R. E. Stratmann, O. Yazyev, A. J. Austin, R. Cammi, C. Pomelli, J. W. Ochterski, R. L. Martin, K. Morokuma, V. G. Zakrzewski, G. A. Voth, P. Salvador, J. J. Dannenberg, S. Dapprich, A. D. Daniels, Ã. Farkas, J. B. Foresman, J. V. Ortiz, J. Cioslowski and D. J. Fox, *Gaussian 09*, Gaussian, Inc., Wallingford, CT, USA, 2009.
21 S. M. Bachrach, *J. Org. Chem.*, 2013, **78**, 10909–10916.
22 L. Goerigk and S. Grimme, *Phys. Chem. Chem. Phys.*, 2011, **13**, 6670–6688.
23 D. J. Knowles and A. J. C. Nicholson, *J. Chem. Phys.*, 1974, **60**, 1180–1181.
24 H. B. Fu, Y. J. Hu and E. R. Bernstein, *J. Chem. Phys.*, 2006, **124**, 24302.
25 M. Kappes and S. Leutwyler, *Atomic and Molecular Beam Methods*, Oxford University Press, 1988, vol. I, pp. 380–415.
26 D. Marx, *ChemPhysChem*, 2006, **7**, 1848–1870.
27 J. F. Garvey, W. J. Herron and G. Vaidyanathan, *Chem. Rev.*, 1994, **94**, 1999–2014.